Bioorganic & Medicinal Chemistry Letters 20 (2010) 3420–3425

Contents lists available at ScienceDirect

Bioorganic & Medicinal Chemistry Letters

journal homepage: www.elsevier.com/locate/bmcl

Novel *C*-aryl glucoside SGLT2 inhibitors as potential antidiabetic agents: Pyridazinylmethylphenyl glucoside congeners

Min Ju Kim, Junwon Lee, Suk Youn Kang, Sung-Han Lee, Eun-Jung Son, Myung Eun Jung, Suk Ho Lee, Kwang-Seop Song, MinWoo Lee, Ho-Kyun Han, Jeongmin Kim, Jinhwa Lee *

Central Research Laboratories, Green Cross Corporation, 303 Bojeong-Dong, Giheung-Gu, Yongin, Gyeonggi-Do 446-770, Republic of Korea

ARTICLE INFO

Article history:
Received 21 December 2009
Revised 3 March 2010
Accepted 3 April 2010
Available online 9 April 2010

Keywords:
SGLT
Dapagliflozin
Pyridazine
Glucoside
Diabetes

ABSTRACT

Novel *C*-aryl glucoside SGLT2 inhibitors containing pyridazine motif were designed and synthesized for biological evaluation. Among the compounds tested, pyridazine containing methylthio moiety **22l** or thiadiazole ring **22ah** showed the best in vitro inhibitory activities in this series (IC_{50} = 13.4, 11.4 nM, respectively) against SGLT2 to date. Subsequently, compound **22l** exhibited reasonable urinary glucose excretion and glucosuria in normal SD rats, thereby demonstrating that this pyridazine series possesses both in vitro SGLT2 inhibition and in vivo efficacy, albeit to a lower degree.

Diabetes has become an increasing concern to the world's population. In 2007, approximately 246 million people were considered diabetic, with an additional 7 million people diagnosed with the disease every year.[1] Diabetes is a chronic metabolic disorder that is defined by the body's inability to generate insulin or the inability of the body to respond adequately to circulating insulin. There are two identified forms of diabetes: type 1 diabetes is distinguished as an autoimmune disease involving pancreatic β-cells, while type 2 diabetes is defined by β-cell dysfunction and insulin resistance.[2] Type 2 diabetes is the most common disorder of glucose homeostasis, accounting for nearly 90–95% of all cases of diabetes.

Sodium-dependent glucose cotransporters (SGLTs) couple the transport of glucose against a concentration gradient with the simultaneous transport of Na^+ down a concentration gradient.[3] Two important SGLT isoforms have been cloned and identified, SGLT1 and SGLT2.[4] SGLT1 is located in the kidney and the heart, where its expression regulates cardiac glucose transport.[5] SGLT1 is a high-affinity, low-capacity transporter and therefore accounts for only a small fraction of renal glucose reabsorption.[6] In contrast, SGLT2 is a low-affinity, high-capacity transporter located exclusively at the apical domain of the epithelial cells in the early proximal convoluted tubule. It is estimated that 90% of renal glucose reabsorption is facilitated by SGLT2; the remaining 10% is likely mediated by SGLT1 in the late proximal straight tubule.[7] Since SGLT2 appears to account for the majority of renal glucose reabsorption based on human mutation studies,[8] it has attracted therapeutic interest.

Extensive SAR studies by Bristol–Myers Squibb identified dapagliflozin **1** (Fig. 1), a potent, selective SGLT2 inhibitor for the treatment of type 2 diabetes.[9–11] At present, dapagliflozin is the most advanced SGLT2 inhibitors in clinical trials and is believed to be the first SGLT2 inhibitor to market.[14] On the other hand, Mitsubishi Tanabe Pharma, in collaboration with Johnson & Johnson, is developing canagliflozin **2** (Fig. 1), another novel *C*-glucoside-derived SGLT2 inhibitor.[12] In August 2009, a phase 3 study was reportedly initiated to evaluate the safety and efficacy of **2** in patients with type 2 diabetes.[13]

In the present study, metabolically more stable *C*-glucosides bearing a heteroaromatic ring were exploited in order to develop novel SGLT2 targeting antidiabetic agents. We envisioned that replacement of the distal ring of dapagliflozin **1** with a heterocyclic ring was a worthy approach for the improvement of the partition coefficient (log *P*) value, to potentially decrease plasma protein binding. For this purpose, the structure of dapagliflozin **1** was modified into compounds bearing a heterocyclic ring. Among a variety of heterocycles, we decided to screen pyridazine as our current efforts. Herein, we report the design, synthesis and biological evaluation of pyridazinylmethylphenyl glucoside congeners.

As shown in Scheme 1, reduction of commercially available 5-bromo-2-chlorobenzoic acid (**4**) with a borane-dimethyl sulfide complex, and subsequent silylation of the corresponding alcohol with TIPSCl (triisopropylsilyl chloride) in the presence of imidazole and DMAP (4-(dimethylamino)pyridine) generated bromide **5** in

* Corresponding author. Tel.: +82 31 260 9892; fax: +82 31 260 9020.
E-mail address: jinhwalee@greencross.com (J. Lee).

0960-894X/$ - see front matter © 2010 Elsevier Ltd. All rights reserved.
doi:10.1016/j.bmcl.2010.04.006

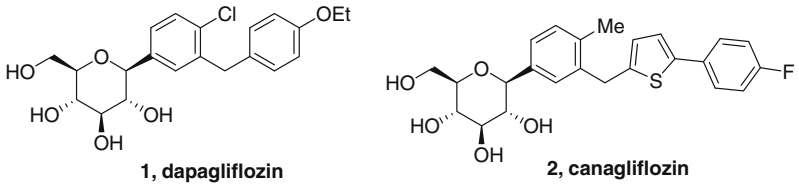

Figure 1. Structures of *C*-aryl glucoside SGLT2 inhibitors.

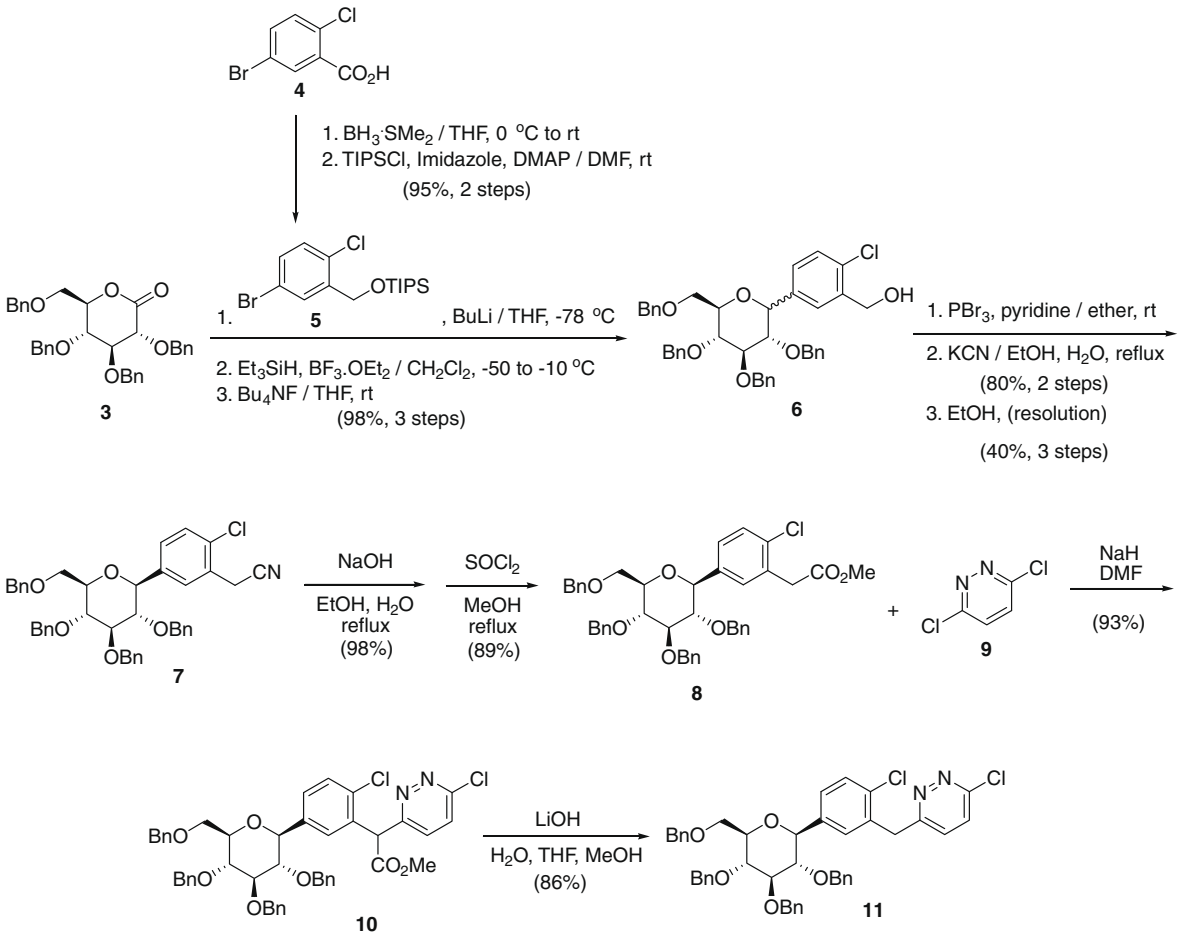

Scheme 1. Preparation of key *C*-glycoside dichloride **11**.

95% yield over two steps. Lithium-halogen exchange, followed by the addition of the nascent lithiated aromatic compound to perbenzylated gluconolactone **3**,[15] produced a mixture of the corresponding lactols. The lactols were reduced using triethylsilane and BF_3 etherate,[14] desilylated and afforded alcohol **6** in 98% yield over the three steps. Thus, alcohol **6** was converted to bromide using PBr_3 in the presence of pyridine, which was treated with KCN in refluxed aqueous EtOH to generate cyanide in 80% yield for the two steps. A mixture of two isomers was resolved through recrystallization from ethanol to produce the required beta-isomer **7** in about 40% yield. Hydrolysis of **7** with sodium hydroxide in aqueous ethanol generated the corresponding carboxylic acid in quantitative yield. Treatment of the carboxylic acid with thionyl chloride in refluxed methanol produced the corresponding methyl ester **8** in 89% yield. Thus, coupling of ester **8** and 3,6-dichloropyridazine (**9**) using NaH in the presence of DMF yielded the corresponding ester **10**, which was hydrolyzed and decarboxylated using lithium hydroxide in an aqueous solution of THF and methanol to generate the key dichloride **11** in 80% yields over two steps.

Utilization of the key intermediate dichloride **11** was illustrated in Scheme 2. Replacement of chloropyridazine with sodium alkoxide provided the corresponding **12**. Likewise, treatment of **11** with NaSMe yielded methylthio-pyridazine **13** in 74% yields uneventfully. Fe(III)-mediated alkylation[21] was conducted on **11** using Grignard reagent such as ethylmagnesium bromide to afford ethylpyridazine **14** in 67% yields. Sonogashira reaction[22] was conducted on **11** with ethynylbenzene **15** to provide the compound **16**. Palladium(0)-catalyzed cyanation[23] proceeded smoothly under microwave irradiation to provide the cyanopyridazine **17**. Suzuki–Miyaura coupling[24] of **11** with boronic acid such as phenylboronic acid **18** to generate phenylpyridazine **19** in 73% yields. Amino group was also introduced smoothly under microwave conditions in approximately 80% yields to produce the compounds.

At last, procedures for deprotection of benzyl groups which were utilized in this article are illustrated in Scheme 3. Thus, the first resort for deprotection is using TMSI (trimethyliodosilane)[16] in acetonitrile as in Case 1 (**13** to **22l**). If the first method fails, use of TMSOTf (trimethylsilyl trifluoromethanesulfonate) in combination with

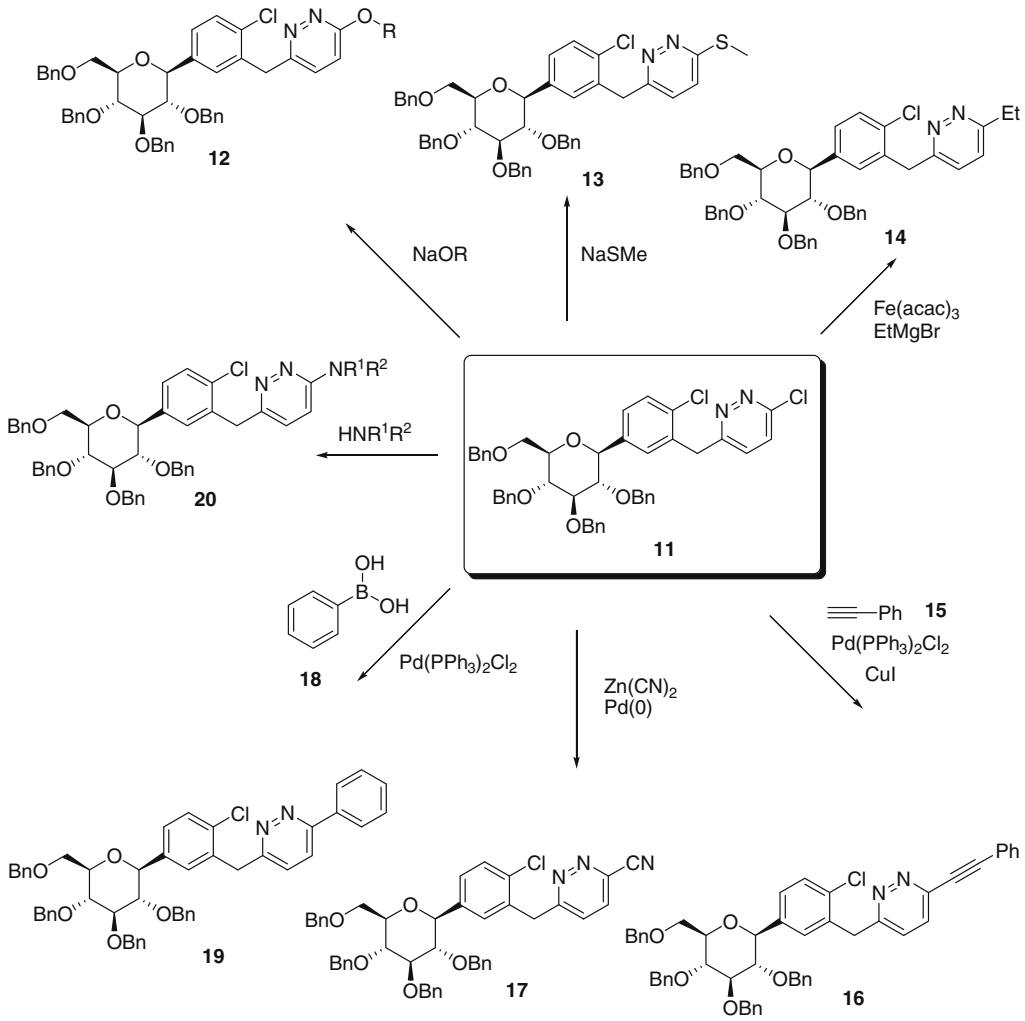

Scheme 2. Preparation of various pyridazines using key *C*-glycoside dichloride **11**.

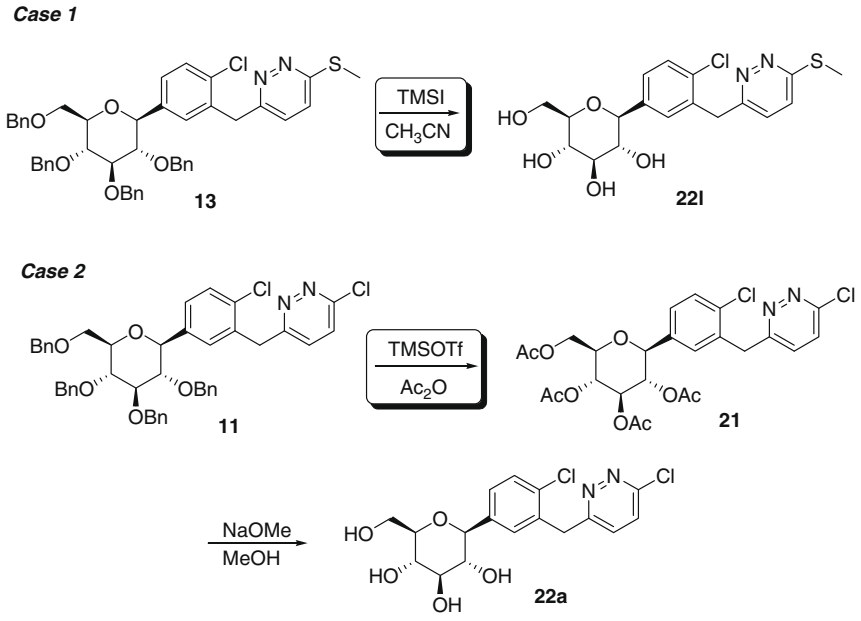

Scheme 3. Debenzylation conditions for the preparation of the target compounds.

Table 1
In vitro inhibitory activity against *h*SGLT2

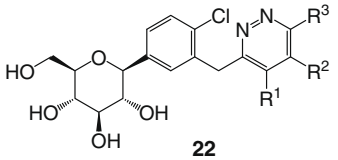

22

unit: nM
Ref. Dapagliflozin (0.49 ± 0.04)[a]

R^1	R^2	R^3	Compound	*h*SGLT2 IC_{50}[b]	R^1	R^2	R^3	Compound	*h*SGLT2 IC_{50}[b]
H	H	Cl	**22a**	202	H	H		**22v**	176
H	H		**22b**	43	H	H		**22w**	64.3
H	H		**22c**	70.8	H	H		**22x**	61.3
H	H		**22d**	110	H	H		**22y**	71.4
H	H	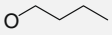	**22e**	109	H	H		**22z**	75.4
H	H		**22f**	435	H	H	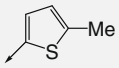	**22aa**	168
H	H	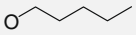	**22g**	17.0	H	H		**22ab**	222
H	H	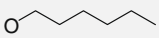	**22h**	17.3	H	H	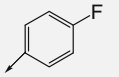	**22ac**	272
H	H	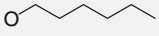	**22i**	50.5	H	H	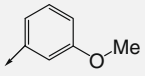	**22ad**	351
H	H		**22j**	111	H	H		**22ae**	64.9
H	H		**22k**	77.6	H	H	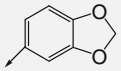	**22af**	82.7
H	H		**22l**	13.4	H	H	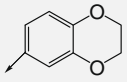	**22ag**	103
H	H		**22m**	71.3	H	H		**22ah**	11.4
H	H		**22n**	1870	H	H	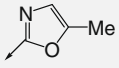	**22ai**	1710
H	H		**22o**	293	H	H		**22aj**	700
H	H		**22p**	131	H	H	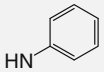	**22ak**	1140
H	H		**22q**	237	H	H		**22al**	1040
H	H		**22r**	259	H	Me		**22am**	1520
H	H		**22s**	356	Me	Me		**22an**	10,000
H	H		**22t**	811				**22ao**	10,000
H	H		**22u**	134					

[a] This data was obtained by multiple determinations.
[b] These data were obtained by single determinations.

acetic anhydride is another option for routine deprotection of benzyl groups as shown in Case 2. For example, **11** was treated with TMSOTf and acetic anhydride[17] to provide the corresponding tetraacetate **21**, then hydrolyzed to yield the target compound **22a**.

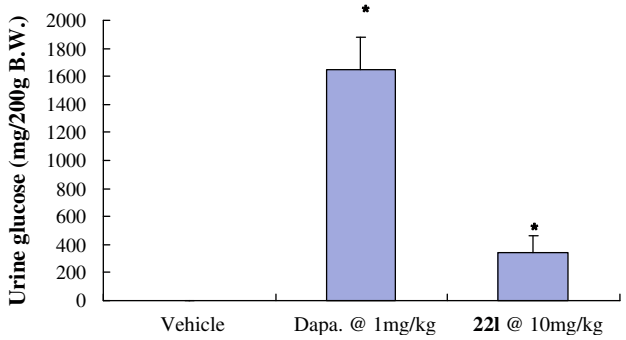

Figure 2. Urinary glucose excretion test of vehicle, compound **1** (1 mg/kg) and **22l** (10 mg/kg) in normal SD rats. All results are expressed as means ± S.E.M. The statistical analysis was performed using a one-way ANOVA followed by the Dunnett's post hoc test. *P <0.05 versus vehicle.

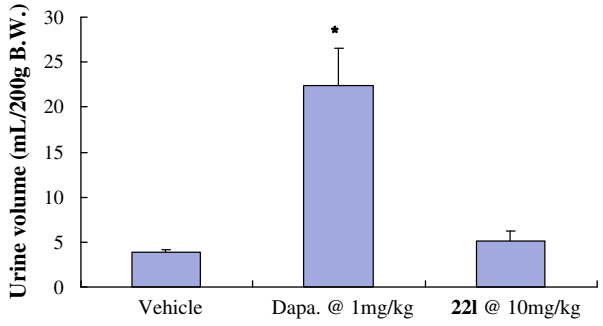

Figure 3. Urine volume excreted of vehicle, compound **1** (1 mg/kg) and **22l** (10 mg/kg) in normal SD rats. All results are expressed as means ± S.E.M. The statistical analysis was performed using a one-way ANOVA followed by the Dunnett's post hoc test. *P <0.05 versus vehicle.

The cell-based SGLT2 AMG (methyl-α-D-glucopyranoside) inhibition assay was performed to evaluate the inhibitory effects of all prepared compounds on *h*SGLT2 activities.[18,19,25,26] Exploration of the SAR began by replacing the phenyl moiety at the distal ring position of dapagliflozin **1** with pyridazine moiety. Table 1 shows the structure–activity relationship upon alteration of the substituent at the distal pyridazine ring employing only the β-anomer. Initially, ethoxide on the pyridazine ring showed reasonable activity (**22b**, IC_{50} = 43 nM). As the size of the carbon chain of alkoxy moiety on pyridazine increases, decrease in the inhibitory activity against *h*SGLT2 is observed up to C-4 chain (**22e**, IC_{50} = 109 nM), but not at C-5 (**22g**, IC_{50} = 17.0 nM) or C-6 (**22h**, IC_{50} = 17.3 nM) before further elongation results in decreased activity as shown in **22i** (IC_{50} = 50.5 nM). Branched alkoxy chains displayed moderate inhibitory activity against *h*SGLT2, showing IC_{50} = 110 nM for **22d** or 435 nM for **22f**, respectively. This pattern is also observed for cyclohexyloxy **22j** (IC_{50} = 109 nM) or pyranyloxy **22k** (IC_{50} = 77.6 nM), suggesting that branched aliphatic chains or slightly increased steric hindrance is not optimal at this position. Replacement for this moiety with methylthio group **22l** improved the inhibitory activity against *h*SGLT2 (IC_{50} = 13.4 nM). However, increase of lipophilicity appeared to deteriorate the activity, showing IC_{50} = 71.3 nM for ethylthio, **22m**, or 1870 nM for phenylthio, **22n**, respectively. Aliphatic chains on the pyridazine ring displayed moderate inhibitory activity, showing IC_{50} = 131–356 nM for **22o**, **22p**, **22q**, **22s**, and **22u**. Again, branched aliphatic chain **22t** showed reduced inhibitory activity against *h*SGLT2. Alkyne **22v** on the pyridazine ring also showed moderate activity against *h*SGLT2 (IC_{50} = 176 nM). Meanwhile, diaryl-types, especially furans, thiophenes or pyridine exhibited more favorable activity (**22w–22z, 22ae**: IC_{50} = 61.3–75.4 nM) than phenyl (**22ab**, IC_{50} = 222 nM). Substitution with bicyclic groups including benzodioxole **22af**, dihydrobenzodioxine **22ag** exhibited modest inhibitory activities against *h*SGLT2 (**22af**, IC_{50} = 82.7 nM; **22ag**, IC_{50} = 103 nM). It is noteworthy that any substitution at the aryl or heteroaryl ring connected with the distal pyridazine ring resulted in products with significantly lower hSGLT2 inhibitory activities (**22ac**, IC_{50} = 272 nM; **22ad**, IC_{50} = 351 nM; **22ai**, IC_{50} = 1.71 μM). Among the biaryl-type compounds tested, thiadiazole **22ah** demonstrated the best in vitro inhibitory activity (IC_{50} = 11.4 nM). However, amine-substituted pyridazines showed weak activities, showing IC_{50} = 700–1140 nM for **22aj**, **22ak**, and **22al**. Moreover, mono- or di-substitution at the pyridazine moiety further deteriorated *h*SGLT2 inhibitory activities, as shown for compounds **22am**, **22n**, and **22ao** (IC_{50} = 1.52 μM, >10 μM, >10 μM, respectively), likely suggesting that increased steric hindrance is not tolerated in the region.

In order to further assess this series, the pharmacokinetic properties of a selected compound, **22l**, were measured in male SD rats. After oral administration of 5 mg/kg of **22l** to rats, a C_{max} of 0.31 μg/mL was obtained at 0.33 h. The elimination half-life of **22l** following oral administration was 1.94 h in rats.[28] Compound **22l** showed decent oral bioavailability (F = 26.1%) in rats. Subsequently, compound **22l** was tested in animal models for in vivo efficacy.[18–20,27] The urine glucose and urine volume data were normalized per 200 g of body weight. As shown in Figure 2, a single oral dose of pyridazine **22l** increased urinary glucose excretion in normal SD rats, resulting in a 180-fold elevation in glucose disposal relative to vehicle controls. Urinary glucose excretion of compounds **1** and **22l** were 1648 ± 228 mg/200 g body weight and 344 ± 116 mg/200 g body weight, respectively (1.90 ± 228 mg/200 g for vehicle). Urine volume excreted in normal SD rats are also shown in Figure 3. Dapagliflozin **1** caused increased urine volume over vehicle in 5.7-fold, while pyridazine **22l** increased urine volume in merely 1.3-fold (vehicle: 3.9 ± 0.23, **1**: 22.36 ± 4.18, **22l**: 5.07 ± 1.09 ml/200 mg body weight, respectively).

Obviously, the decreased in vivo efficacy of the current SGLT2 inhibitor **22l** compared with dapagliflozin **1** could be attributed to the difference in inherent in vitro potencies (**22l**: IC_{50} = 13.4 nM vs **1**: IC_{50} = 0.49 nM) as well as in pharmacokinetic properties. Thus, replacement of the distal ring of dapagliflozin **1** with a pyridazine ring as in compound **22l** appeared to diminish the in vitro activity and oral absorption, thereby resulting in the diminished in vivo efficacy in animal models.

In summary, metabolically more stable *C*-glucosides bearing pyridazine ring as a potential antidiabetic agent were exploited. Among the compounds tested, pyridazine containing methylthio moiety **22l** or thiadiazole ring **22ah** showed the best in vitro inhibitory activities against *h*SGLT2 in this series to date (IC_{50} = 13.4, 11.4 nM, respectively). Subsequently, compound **22l** demonstrated reasonable urinary glucose excretion and glucosuria in normal SD rats, thereby demonstrating that this pyridazine series possesses both in vitro SGLT2 inhibition and in vivo efficacy, albeit to a relatively lower degree. The information acquired from this series of compounds can be utilized as a quick reference to achieve more advanced series in this area.

Acknowledgments

We appreciate Dr. Chong-Hwan Chang for his leadership and dedication during his tenure as Head of R&D, Green Cross Corporation (GCC).

Supplementary data

Supplementary data associated with this article can be found, in the online version, at doi:10.1016/j.bmcl.2010.04.006.

References and notes

1. International Diabetes Federation, Diabetes Atlas, 3rd ed., International Diabetes Federation, Brussels, Belgium, 2006.
2. Dwarakanathan, A. *J. Insur. Med.* **2006**, *38*, 20.
3. Mackenzie, B.; Loo, D. D. *J. Biol. Chem.* **1996**, *20*, 32678.
4. Wright, E. M. *Am. J. Physiol.* **2001**, *280*, F10.
5. Zhou, L.; Cryan, E. V.; D'Andrea, M. R.; Belkowski, S.; Conway, B. R.; Demarest, K. T. *J. Cell. Biochem.* **2003**, *90*, 339.
6. Evans, S.; Grasset, E.; Heyman, M.; Dumonitier, A. M.; Beau, J. P.; Desjeux, J.-F. *J. Pediatr. Gastroenterol. Nutr.* **1985**, *4*, 878.
7. Moe, O. W.; Berry, C. A.; Rector, F. C. In *The Kidney*; Brenner, B. M., Rector, F. C., Eds., 5th ed.; WB Saunders Co.: Philadelphia, 2000; pp 375–415.
8. van den Heuvel, L. P.; Assink, K.; Willesen, M.; Monnens, L. *Hum. Genet.* **2002**, *111*, 544.
9. Ellsworth, B. A.; Meng, W.; Patel, M.; Girotra, R. N.; Wu, G.; Sher, P.; Hagan, D.; Obermeier, M.; Humphreys, W. G.; Robertson, J. G.; Wang, A.; Han, S.; Waldron, T.; Morgan, N. N.; Whaley, J. M.; Washburn, W. N. *Bioorg. Med. Chem. Lett.* **2008**, *18*, 4770.
10. Meng, W.; Ellsworth, B. A.; Nirschl, A. A.; McCann, P. J.; Patel, M.; Girotra, R. N.; Wu, G.; Sher, P. M.; Morrison, E. P.; Biller, A. A.; Zahler, R.; Deshpande, P. P.; Pullockaran, A.; Hagan, D. L.; Morgan, N.; Taylor, J. R.; Obermeier, M. T.; Humphreys, W. G.; Khanna, A.; Discenza, L.; Robertson, J. G.; Wang, A.; Han, S.; Wetterau, J. R.; Janovitz, E. B.; Flint, O. P.; Whaley, J. M.; Washburn, W. N. *J. Med. Chem.* **2008**, *51*, 1145.
11. Washburn, W. N. *J. Med. Chem.* **2009**, *52*, 1785.
12. Nomura, S.; Sakamaki, S.; Hongu, M.; Kawanski, E.; Koga, Y.; Sakamoto, T.; Yamamoto, Y.; Ueta, K.; Kimata, H.; Nakayama, K.; Tsuda-Tsukimoto, M. Presented at the 238th American Chemical Society National Meeting and Exposition, Washington, DC, August 16–20, 2009; Medi-151.
13. Johnson & Johnson Pharmaceutical, www.clinicaltrials.gov, 2009, NCT00968812.
14. Ellsworth, B. A.; Doyle, A. G.; Patel, M.; Caceres-Cortes, J.; Meng, W.; Deshpande, P. P.; Pullockaran, A.; Washburn, W. N. *Tetrahedron: Asymmetry* **2003**, *14*, 3242.
15. (a) Kraus, G. A.; Molina, M. T. *J. Org. Chem.* **1998**, *53*, 752; (b) Xie, J.; Durrant, F.; Valery, J.-M. *J. Org. Chem.* **2003**, *68*, 7896.
16. Jung, M. E.; Lyster, M. A. *J. Org. Chem.* **1997**, *42*, 3761.
17. Angibeaud, P.; Utile, J.-P. *Synthesis* **1991**, 737.
18. Han, S.; Hagan, D. L.; Taylor, J. R.; Xin, L.; Meng, W.; Biller, S. A.; Wetterau, J. R.; Washburn, W. N.; Whaley, J. M. *Diabetes* **2008**, *57*, 1723.
19. Katsuno, K.; Fujimori, Y.; Takemura, Y.; Hiratochi, M.; Itoh, F.; Komatsu, Y.; Fujikura, H.; Isaji, M. *J. Pharmacol. Exp. Ther.* **2007**, *320*, 323.
20. Arakawa, K.; Ishihara, T.; Oku, A.; Nawano, M.; Ueta, K.; Kitamura, K.; Matsumoto, M.; Saito, A. *Br. J. Pharmacol.* **2001**, *132*, 578.
21. Furstner, A.; Leitner, A.; Mendez, M.; Krause, H. *J. Am. Chem. Soc.* **2002**, *124*, 13856.
22. Sonogashira, K.; Tohda, Y.; Hagihara, N. *Tetrahedron Lett.* **1975**, 4467.
23. Chen, C.-y.; Frey, L. F.; Shultz, S.; Wallace, D. J.; Marcantonio, K.; Payack, J. F.; Vazquez, E.; Springfield, S. A.; Zhou, G.; Liu, P.; Kieczykowski, G. R.; Chen, A. M.; Phenix, B. D.; Singh, U.; Strine, J.; Izzo, B.; Krska, S. W. *Org. Process Res. Dev.* **2007**, *11*, 616.
24. Miyaura, N.; Suzuki, A. *Chem. Rev.* **1995**, *95*, 2457.
25. For cloning and cell line construction for human SGLT2, human SGLT2 (*h*SGLT2) gene was amplified by PCR from cDNA-Human Adult Normal Tissue Kidney (Invitrogen, Carlsbad, CA). The *h*SGLT2 sequence was cloned into pcDNA3.1(+) for mammalian expression and were stably transfected into chinese hamster ovary (CHO) cells. SGLT2-expressing clones were selected based on resistance to G418 antibiotic (Geneticin®, Invitrogen, Carlsbad, CA) and activity in the ^{14}C-α-methyl-D-glucopyranoside (^{14}C-AMG) uptake assay.
26. For sodium-dependent glucose transport assay, cells expressing *h*SGLT2 were seeded into a 96-well culture plate at a density of 5×10^4 cells/well in RPMI medium 1640 containing 10% fetal bovine serum. The cells were used 1 day after plating. They were incubated in pretreatment buffer (10 mM HEPES, 5 mM Tris, 140 mM choline chloride, 2 mM KCl, 1 mM $CaCl_2$, and 1 mM $MgCl_2$, pH 7.4) at 37 °C for 10 min. They were then incubated in uptake buffer (10 mM HEPES, 5 mM Tris, 140 mM NaCl, 2 mM KCl, 1 mM $CaCl_2$, 1 mM $MgCl_2$, and 1 mM ^{14}C-nonlabeled AMG pH 7.4) containing ^{14}C-labeled (8 μM) and inhibitor or dimethyl sulfoxide (DMSO) vehicle at 37 °C for 2 h. Cells were washed twice with washing buffer (pretreatment buffer containing 10 mM AMG at room temperature) and then the radioactivity was measured using a liquid scintillation counter. IC_{50} was determined by nonlinear regression analysis using GraphPad PRISM.[20,21]
27. For urinary glucose excretion in normal animal: urinary glucose excretion was evaluated on normal Sprague-Dawley (SD) rats.[20–22] Male SD rats weighing 250–300 g (7–8 weeks old) were purchased from Orient-Bio Laboratory Animal Research Center Co. (Gyeonggi-do, Korea). They were housed in a temperature (25 ± 2 °C), and moisture (55 ± 10%) controlled room, exposed to a controlled 12 h cycle of light and darkness, and allowed free access to food and water. All animals were acclimated for one week prior to the experiment. For glucosuria assessment, overnight-fasted SD rats were placed into metabolism cages for baseline urine collection over 24 h. Rats were weighed, randomized into three groups in plane (n = 3), dosed orally with single doses of vehicle or drug (**1** @1 mg/kg, **32l** @10 mg/kg), and subsequently dosed orally with 50% aqueous glucose solution (2 g/kg). Immediately after dosing, rats were returned to the metabolism cages for 24 h urine collection and re-fed at 1 h after the glucose challenge.
28. For comparison, after oral administration of 5 mg/kg of **1** to rats, a C_{max} of 2.50 μg/mL was obtained at 0.67 h. The elimination half-life of **1** following oral administration was 4.01 h in rats. Compound **1** showed desirable oral bioavailability (F = 88.42%) in rats.